Annual General Conference
Assemblée générale annuelle

Edmonton, Alberta
June 6-9, 2012 / *6 au 9 juin 2012*

Coupling of Random Field Theory and the Discrete Element Method in the Reliability Analysis of Geotechnical Problems

V. D. H. Tran, M. A. Meguid, L.E. Chouinard
Department of Civil Engineering and Applied Mechanics, McGill University

Abstract: An efficient algorithm to create discrete element samples with predefined properties incorporating the random field theory is introduced in this paper. The algorithm considerably reduces the time needed to generate a large scale domain as only a small initial sample with dynamic packing is used. Three-dimensional anisotropic random fields are generated using the Local Average Subdivision (LAS) method accounting for the spatial variability. The random fields are then mapped on the discrete element domain and uncertain parameters of each particle are obtained from the corresponding random field cell. Triaxial tests are conducted on large soil samples with the dimensions of 1.5m x 3.0m x 1.5m comprising over 150,000 spherical particles. The normal and tangential stiffnesses of the particles are selected as random variables since they have a significant effect on the soil behavior under triaxial testing conditions. Monte Carlo simulation is implemented to analyze the probabilistic features of the output values. The results of parametric studies are also presented.

1. Introduction

Soil properties at each location within the soil mass are considered to be random variables and typically exhibit considerable variation from point to point. Therefore, it is essential to consider the spatial variability of the soil domain. Neglecting the spatial variability may lead to the underestimation or overestimation of the probability of unsatisfactory performance. Traditional methods often neglect the spatial variability or consider it in approximate ways. Popular methods such as the First-Order Second Moment Method and the First-Order Reliability Method do not consider the spatial variability. Moreover, they have some other limitations regarding their approximate assumptions of performance function derivation. Although the Point Estimate Method is being widely used in geotechnical engineering, it still neglects the spatial variability and does not provide detailed information of the output distribution.

Numerical methods have been intensively implemented to solve complicated geotechnical problems with nonlinear and implicit performance function and recent development in numerical methods has made it more feasible to combine reliability analysis with numerical simulations. Schweiger et al. (2001) proposed a framework in which the Point Estimate Method was used in conjunction with the deterministic Finite Element Method to analyze the probabilistic behavior of a sheet-pile wall and tunnel excavation process. Although this approach accounts for soil variability in the deterministic finite element method, it does not consider the spatial variability of soil properties. Schweiger and Peschl (2005) used the Random Set Finite Element Method to take into account the spatial correlation in an approximate way. However, spatial variation can be better represented by random field theory. The Random Finite Element Method proposed by Griffiths and Fenton (1993) which combines random field theory and Monte-Carlo simulation has been successfully used for some geotechnical problems such as bearing capacity, settlement, pillar stability, steady seepage and slope stability.

An alternative numerical method that can be used for geotechnical problems is the Discrete Element Method (DEM). The method proposed by Cundall and Strack (1979) has proven to be a versatile approach for the simulation of granular materials. This method can overcome difficulties that can not be fully solved using the Finite Element Method, especially those related to the behavior of granular soils under large deformations. Suchomel and Mašin (2010) suggested that random field theory can be combined with the DEM. This method, however, has hardly been applied in conjunction with reliability analysis partly due to the large computational time required and the limitation of current computer capacity. Hsu and Nelson (2006) used this approach for the slope stability analysis of weak rock masses. The spatial variability of material properties was considered with random field elements embedded in the numerical analyses. The rock mass was simulated using two dimensional (2D) discrete elements with a maximum of 10 different material properties available in the UDEC program. This limitation did not allow a proper representation of the spatial variability of material properties.

There are several issues that have to be considered when implementing reliability analysis with the DEM: (1) spatial variability has to be considered in the discrete element model to represent real condition, (2) the total computational time required for the packing process of a large-scale model should be acceptable, and (3) the random field of material properties has to be mapped onto the discrete element domain defined by the packing algorithm. This paper presents an algorithm that satisfies these criteria.

In this study, the packing algorithm suggested by Dang and Meguid (2010) is adopted since it allows for the generation of three-dimensional (3D) packing models with pre-defined properties and the time required to create large-scale domains is reduced considerably. The particle domain obtained with this technique is meshed into a user-defined 3D grid to which the anisotropic random fields are assigned using the Local Average Subdivision Method (LAS) proposed by Fenton and Vanmarcke (1990). Triaxial test simulations are performed to demonstrate the effect of material variability on the behavior of soil samples.

2. Generation of the Particle Domain

2.1 Packing Algorithm

The packing procedure consists of two phases: in phase 1, a relatively small size initial packing is first generated with a predefined grain size distribution and target porosity. The final packing is then generated in phase 2 by assembling the small samples using the “flip technique” to maintain the same grain size distribution and porosity (Dang and Meguid 2010).

The details of each phase are as follow:

Phase 1: The dimensions of a box for the initial packing are denoted in the x, y and z directions as (b_x x b_y x b_z). A number of non-overlapping particles are then generated inside the box with the dimensions of (b_x x h_y x b_z) where the height h_y of the box is larger than b_y to ensure that all particles can settle under gravity into the box. Additional particles are generated until the target volume of all particles is reached.

In order to obtain the initial packing with a predefined particle size distribution, the radius of a particle i is randomly generated from the grain size distribution:

$$[1] \quad r_i = [D_1 + (RAN_i \times 100 - P_1) \times \frac{(D_2 - D_1)}{(P_2 - P_1)}]/2$$

where r_i is the radius of particle i, RAN_i is a uniformly distributed random number generated in the range $0 \leq RAN_i < 1$, P_1 and P_2 are the percentage of grains (%) passing through sieves S_1 and S_2 such that $P_1 \leq 100.RAN_i < P_2$, sieve S_1 and S_2 are then specified by P_1 and P_2, D_1 and D_2 are the

diameters of sieves S_1 and S_2. After the packing reaches the stability condition, it is still a loose structure. A compaction procedure with a combination of shaking and vertical compression is applied in order to obtain the target porosity. Phase 1 continues until the initial packing satisfies the stability condition.

Phase 2: The "flip technique" is implemented in this phase to overcome the large amount of computation associated with the dynamic packing method. The technique is a 3D process and is illustrated in Figure 1:

The final packing space with the dimensions of (p_x x p_y x p_z) is divided into (n_x x n_y x n_z) domains. An initial packing S_0 (b_x x b_y x b_z) generated using the technique described in phase 1 is cloned repeatedly to obtain a final packing with similar properties. All particles which were initially in contact with the walls now become in contact with other particles in the final packing.

The initial packing S_0 is first placed into the lower left corner of the domain. Block S_{yz}, obtained by flipping S_0 around the y-z plane, is placed to the right of sample S_0. A second sample S_0 is then placed to the right of S_{yz} and the process is repeated until the first row is completed. The entire first row is then flipped around the x-z plane in a similar process to obtain the second row, and the process is repeated to generate the first slice consisting of (n_x x n_y) small blocks in n_x columns and n_y rows. The first slice is flipped around the x-y plane to generate the second slice, and the final packing is obtained by repeating the process. Finally, the final packing is allowed to reach the stability condition.

In order to identify the position of a particle in the soil sample grid, each particle is marked by the block from which it is generated. A block that is of slice k, row j and column i within that row is noted as (i, j, k); all spheres of that block are then identified by (i, j, k).

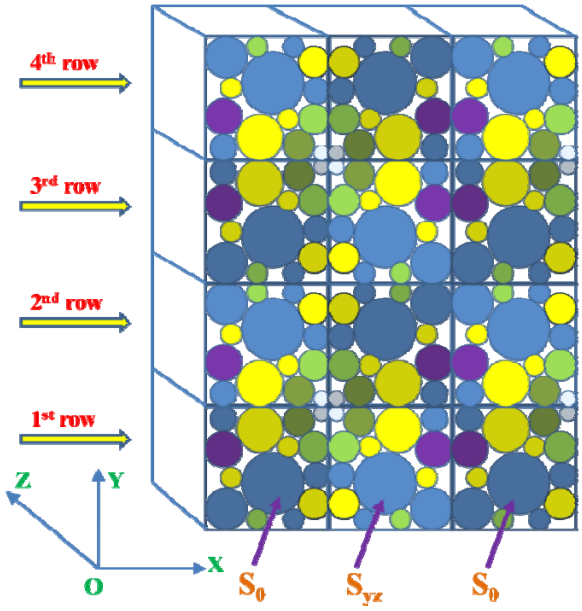

Figure 1: Flip technique to obtain the final packing

2.2 Packing Process

The above packing algorithm is used to generate a soil sample, which has the dimensions of 1.5m width, 3.0m height and 1.5m depth. The soil mass is formed from 6 x 12 x 6 = 432 small initial blocks, each block is cubic with the dimensions of 0.25m x 0.25m x 0.25m.

A simple contact law is applied in this study to calculate contact forces. The force vector $\vec{F}$ which represents the interaction between two particles is decomposed into normal and tangential forces:

[2] $$\vec{F}_n = K_n.\vec{\Delta}_n, \delta\vec{F}_s = -K_s.\delta\vec{\Delta}_s$$

Where $\vec{F}_n$ and $\vec{F}_s$ are the normal and tangential forces; K_n and K_s are the normal and tangential stiffnesses at the contact; $\delta\vec{\Delta}_s$ is the incremental tangential displacement and $\vec{\Delta}_n$ is the normal penetration between the two particles.

K_n and K_s are defined by the following equations:

[3] $$K_n = r\frac{k_n^A.k_n^B}{k_n^A + k_n^B}, K_s = r\frac{k_s^A.k_s^B}{k_s^A + k_s^B}$$

where k_n and k_s are the normal and tangential stiffnesses of two contact particles A and B, respectively; r is the average radius of the two particles.

The particles are assumed to have properties of granular material with no cohesion. The target porosity of the sample is 0.40. The target grain size distribution is given in Table 1 and the material properties of the particles during the packing process are given in Table 2.

Table 1: Grain size distribution

Sieve diameter (mm)	% passing (number)
10	0
20	0
40	31.47
100	90.93
160	99.64
200	100

Table 2: Material properties for the packing process

Parameter	Value
Particle density (kg/m^3)	2600
Particle normal stiffness k_n (Pa)	9 x 10^8
Ratio k_s/k_n	0.1
Friction angle φ (degrees)	32
Box's Poisson's ratio	0.2
Box's friction (degrees)	0

3. Random Field Generator

Several approaches have been proposed to generate spatially varying random fields including the Turning Bands Method, the Cholesky decomposition technique and the Local Average Subdivision Method (Fenton and Vanmarcke 1990). The LAS method has been chosen in this study as it allows for the implementation in numerical methods. In addition, it generates a discrete grid of local averages of a standard Gaussian random field and represents a random field accurately even for coarse meshes.

In this study, the normal stiffness k_n and the tangential stiffness k_s of particles are assumed to be random variables since they have a great influence on the behavior of soil samples (Belheine et al. 2009). The normal and tangential stiffnesses are assumed to follow lognormal distributions. Since the cross correlation between k_n and k_s is usually not well known, the two stiffnesses are assumed to be perfectly correlated for the sake of simplicity. The ratio k_s/k_n is kept constant for all particles, which means only the random field of k_n is initially generated by the random field generator and the random field of k_s is obtained directly from k_n.

The distribution of k_n is characterized by the mean μ_{k_n}, the standard deviation σ_{k_n} and the correlation lengths. A log-normally distributed random field of k_n is given by:

[4] $$k_n(\tilde{x}_i) = \exp\{\mu_{lnk_n} + \sigma_{lnk_n} G_{lnk_n}(\tilde{x}_i)\}$$

where $\tilde{x}_i$ is the spatial position at which k_n is desired; $G_{lnk_n}(\tilde{x}_i)$ is a normally distributed random field with zero mean, unit variance and given correlation lengths.

The two parameters μ_{lnk_n} and σ_{lnk_n} are obtained from the lognormal distribution transformations:

[5] $$\sigma^2_{lnk_n} = \ln(1 + COV^2_{k_n}),\ \mu_{lnk_n} = \ln\mu_{k_n} - \frac{1}{2}\sigma^2_{lnk_n}$$

where COV_{k_n} is the coefficient of variation of k_n.
The random field $G_{lnk_n}(\tilde{x}_i)$ is generated using the 3-D Markovian correlation function:

[6] $$\rho = \exp\left(-\sqrt{\left(\frac{2\tau_x}{\theta_{lnk_n}(x)}\right)^2 + \left(\frac{2\tau_y}{\theta_{lnk_n}(y)}\right)^2 + \left(\frac{2\tau_z}{\theta_{lnk_n}(z)}\right)^2}\right)$$

where τ_x, τ_y and τ_z are the three components of the distance between two points in the random field; $\theta_{lnk_n}(x)$, $\theta_{lnk_n}(y)$ and $\theta_{lnk_n}(z)$ are the correlation lengths in x, y and z direction. These correlation lengths account for the anisotropic character of the random field and represent the distance over which the spatially random variables tend to have significant correlation. The horizontal correlation length is chosen greater than the vertical due to the fact that soil generated from a deposition process has strong variability in the vertical direction. It should be noted that the spatial correlation structure of soil domains, especially in the horizontal direction is usually not well known and requires a large amount of site exploration which is not always feasible. Therefore, the vertical correlation length is varied in this study from 0.01 m (much smaller than the soil sample size) to 10.0 m (larger than the soil sample size) and the horizontal correlation length is kept 10 times greater than the vertical; the value of COV_{k_n} is ranged from 0.4 to 2.0 while the mean value is kept constant as shown in Table 3.

In order to assign different realizations of the random field to the discrete element grid, the random field grid is made identical to the grid of the soil sample. Each random field is composed of 6 x 12 x 6 cells in the x, y and z direction, respectively. The dimensions of each cell are 0.25m x 0.25m x 0.25m, which are the same size as the initial packing of the sample.

Table 3: Probabilistic description for the random variables

Parameter	Value
Type of distribution	Lognormal
Mean μ_{k_n} (Pa)	9×10^8
COV_{k_n}	0.4, 0.8, 1.2, 1.6, 2.0
Vertical correlation length $\theta_{lnk_n}(y)$ (m)	0.01, 0.1, 0.5, 1.0, 10.0
Horizontal correlation length $\theta_{lnk_n}(x) = \theta_{lnk_n}(z)$ (m)	0.1, 1.0, 5.0, 10.0, 100.0

4. Numerical Simulation

Both the packing algorithm and the random field generator were implemented inside the open source code YADE (Kozicki and Donze 2008) to generate random soil samples. As the main purpose of this study is to examine the spatial variability of k_n and k_s, generated random samples should allow for the variability of k_n and k_s while keeping other parameters constant. Since the random generation of particles is used in the packing procedure to maintain the structure of the final packing, the final assembly is obtained by executing the packing procedure only once using the mean value of k_n and k_s.

In the first phase of the packing process, an initial packing that consists of 351 particles is generated. The porosity of the initial packing at the end of phase 1 is 0.395 which is close to the target porosity of 0.40. The expected grain size distribution of the packing is also achieved using Eq. 1. The final packing comprises 151,632 particles at the end of the second phase of the packing procedure and the properties of the initial packing are preserved through the flipping and cloning process. It can be seen from Figure 2 that the stresses σ_{xx}, σ_{yy} and σ_{zz} in the x, y and z directions generally satisfy the expected geostatic stress distribution. Note that the dynamic packing procedure is applied only for the initial sample, and therefore, the total simulation time is greatly reduced. The entire packing process which requires nearly 72 hours using a personal computer is rather efficient compared to the time that would be required for packing a similar sample with over 150,000 particles.

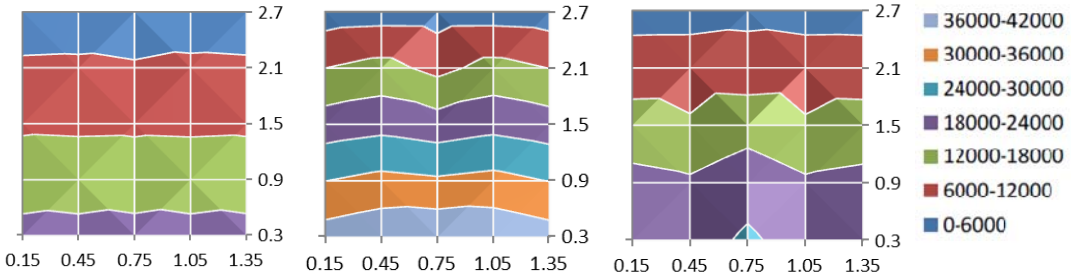

Figure 2: Contours of the stress distribution (in Pa)

The random field generator is then activated to generate several hundred sets of random fields for the normal stiffness k_n which are mapped on the final sample created by the packing process. Note that each sphere in the soil sample is marked by its identification generated from phase 2 of the packing procedure and the grid of the random field is identical to the grid of the soil sample, making it possible to connect the sphere with its corresponding random cell. The normal stiffness of each spherical particle is re-assigned the value of its corresponding random field cell, and the tangential stiffness k_s is set as a function of the specified ratio k_s/k_n. Particles that are created in the same block are assigned the same values for k_n and k_s.

Figure 3b and 3c show two typical soil samples corresponding to $\theta_{\ln k_n}(y) = 1.0\,\mathrm{m}$ and $\theta_{\ln k_n}(y) = 0.1\,\mathrm{m}$ as large and small correlation lengths, respectively. Lighter shaded regions indicate smaller k_n while darker shaded regions indicate larger k_n. The effect of the correlation lengths is also evident: the smaller correlation lengths of the sample in Figure 3c leads to larger spatial variation of k_n compared to the sample in Figure 3b. In both cases, the larger horizontal correlation length results in more uniform k_n in the horizontal direction compared to the vertical direction.

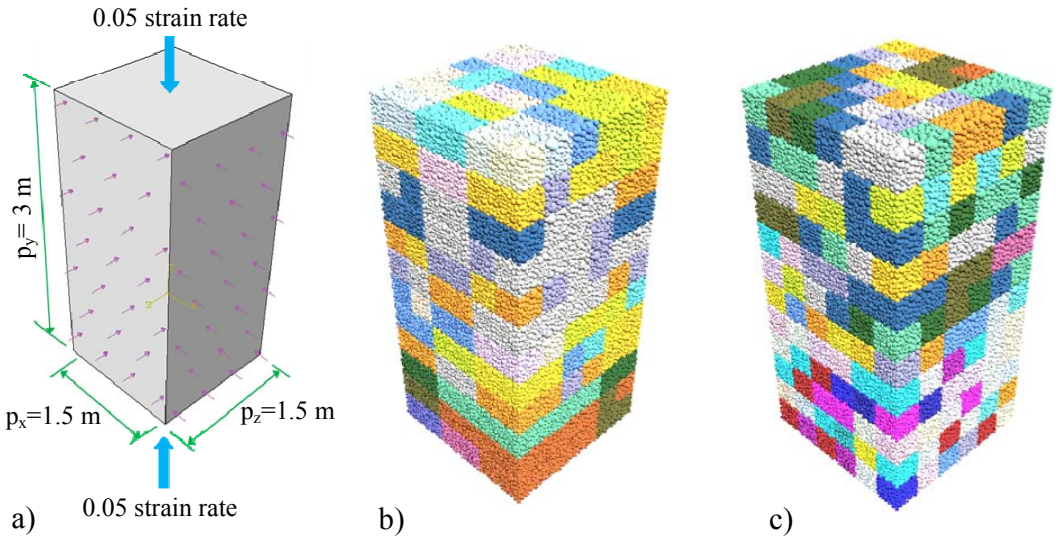

Figure 3: (a) Soil sample configuration. (b) A random soil sample with $\theta_{\ln k_n}(y) = 1.0\,\mathrm{m}$ (c) A random soil sample with $\theta_{\ln k_n}(y) = 0.1\,\mathrm{m}$

The effects of the variability of material properties are analyzed using Monte Carlo simulation. Numerical triaxial tests are performed on the randomly generated soil samples to analyze the probabilistic properties of the response. In each triaxial test, the sample is first compressed isotropically under a specified confining pressure. After the stability condition is reached, an additional strain rate of 0.1 is applied to the top surface while the pressures on the side walls are kept constant. The confining stress of 100 kPa is used in the analysis.

It can be seen from deterministic studies that the modulus E_{50} of the sample, which is obtained from the axial strain - deviator stress relationship at 50% of the maximum deviator stress, is highly dependent on the microscopic parameter k_n. Consequently the probabilistic analysis in this paper is performed related to this value. Note that if the packing procedure is used every time k_n is changed, soil samples with different packing structures are obtained and the macro-micro relationship may be different. The importance of the packing structure on the macro-micro relationship is beyond the scope of this study.

For each case of analysis, Monte Carlo simulations were performed for 250 realizations of random fields followed by the discrete element analysis of triaxial tests. Note that the number of realizations is limited by the execution time required for a single run (a numerical triaxial test requires about 5 hours on a personal computer with Core i7 Processor 2.8 GHz). It is seen that the mean and standard deviation are quite stable for the sample size of 250.

5. Probabilistic Analyses

5.1 Distribution Fitting

A histogram of E_{50} is shown in Figure 4a. The shape of the histogram suggests a lognormal distribution. The fitted lognormal distribution, with parameters defined by the mean μ_{E50} and the standard deviation σ_{E50}, is given in the histogram. A statistical analysis indicates a good fit when a lognormal distribution is assumed. Both the Chi-Square goodness-of-fit test (p-value of 69.4%)

and the P-P plot demonstrate that the lognormal distribution is a good choice for the modulus E_{50} (Figure 4b). This is to be expected since the input random parameters k_n and k_s are log-normally distributed.

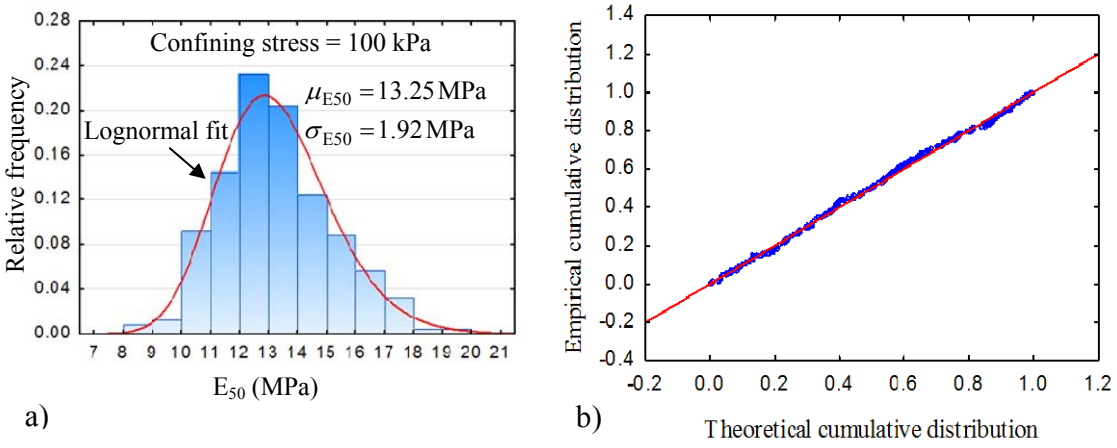

Figure 4: (a) A histogram of modulus E_{50}. (b) Probability-Probability (P-P) plot for lognormal distribution fitting ($COV_{k_n} = 0.8, \theta_{\ln k_n}(y) = 1.0\,m$)

5.2 Parametric Studies

As shown in Figure 5, the mean of E_{50} decreases for all correlation lengths when the coefficient of variation of k_n increases. This reduction implies that the macroscopic modulus is smaller than the deterministic modulus when spatial variability of soil properties is considered. μ_{E50} is also depends on correlation lengths. The maximum value of μ_{E50} is obtained at an intermediate vertical correlation length of about 0.5 m. It can be hypothesized that this vertical correlation length results in a "rough" soil domain with high macroscopic modulus while larger or smaller correlation lengths lead to smaller macroscopic modulus. When $\theta_{\ln k_n}(y) \to 0$, the local averaging causes k_n to tend to its median which is $\exp(\mu_{\ln k_n})$ everywhere in the domain. For the case $\theta_{\ln k_n}(y) \to \infty$, there is no local averaging and the soil properties are spatially constant for each realization while varying from realization to realization. The mean value μ_{E50} in this case can be calculated with k_n selected randomly from a lognormal distribution with a given mean and standard deviation.

Figure 6 illustrates the variation of the standard deviation of E_{50} as a function of COV_{k_n} and $\theta_{\ln k_n}(y)$. σ_{E50} increases with the rise of COV_{k_n} and $\theta_{\ln k_n}(y)$, and the largest value is achieved when $\theta_{\ln k_n}(y) \to \infty$. Due to the local averaging, the standard deviation of E_{50} decreases when the correlation lengths are reduced. When $\theta_{\ln k_n}(y) \to 0$, the variance of k_n tends to zero since the local averaging results in a constant value for each simulation.

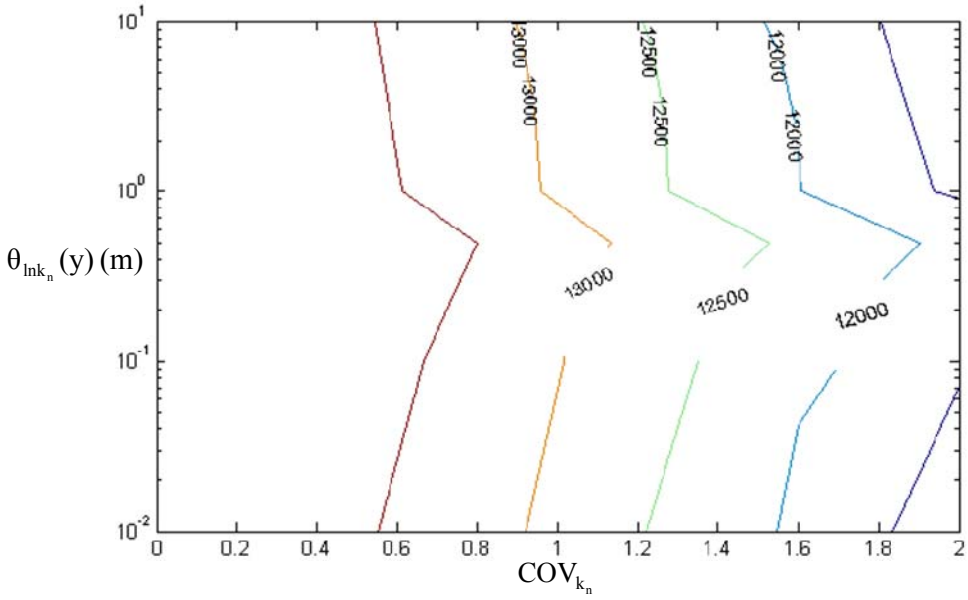

Figure 5: Variation of μ_{E50} with COV_{k_n} and $\theta_{\ln k_n}(y)$

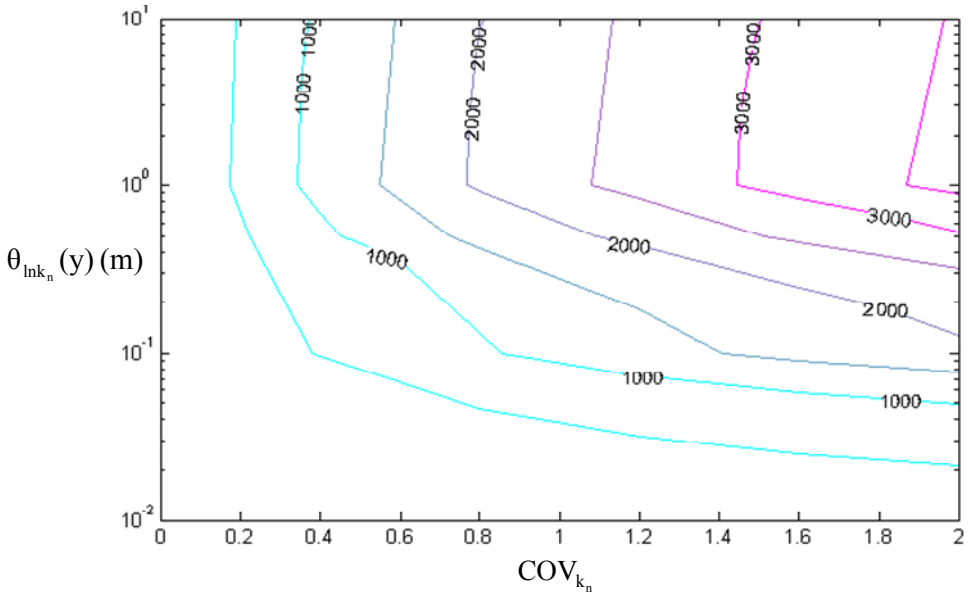

Figure 6: Variation of σ_{E50} with COV_{k_n} and $\theta_{\ln k_n}(y)$

6. Summary and Conclusions

In this study, a framework to combine random field theories and the discrete element method to analyze the behavior of soil structures under spatially varying properties was presented. A triaxial testing of spatially varying soil samples with anisotropic, log-normally distributed random fields was performed. Using Monte Carlo simulation, histograms and type of distributions for output parameters were discussed. It was seen that lognormal distribution is a good approximation for the macroscopic modulus E_{50}.

As the coefficient of variation of the particle normal stiffness increases, the expected macroscopic modulus decreases while the standard deviation and the coefficient of variation tend to rise. Increasing the correlation lengths also leads to the positive behavior of the standard deviation of E_{50}. The mean of E_{50}, on the other hand, rises from small values of correlation lengths to its peak value at the vertical correlation length $\theta_{\ln k_n}(y)$ of about 0.5 m and then falls as $\theta_{\ln k_n}(y)$ is greater than 0.5 m.

The algorithm has some advantages in creating 3D discrete element domains accounting for the spatial variability of the properties. The time required to create a 3D soil sample is greatly reduced, 3D random fields of soil properties which are anisotropic and spatially varied can be easily mapped on the soil domain, and the 3D random field generator is embedded into the discrete element code. The proposed algorithm has proved to be efficient and can be implemented to solve other geotechnical problems by coupling reliability analysis and the discrete element method.

Acknowledgments

This research is supported by a research grant from the Natural Sciences and Engineering Research Council of Canada (NSERC). The financial support provided by McGill Engineering Doctoral Award (MEDA) to the first author is greatly appreciated.

References

Belheine, N., Plassiard, J.P., and Donze´, F.V. 2009. Numerical simulation of drained triaxial test using 3D discrete element modeling. *Computers and Geotechnics*, 36:320-331.

Cundall, P. and Strack, O.D. 1979. A discrete numerical model for granular assemblies. *Geotechnique*, 29(1):47-65.

Dang, H.K. and Meguid, M.A. 2010. Algorithm to generate a discrete element specimen with predefined properties. *International Journal of Geomechanics*, 10(2):85-91.

Fenton, G.A. and Vanmarcke, E.H. 1990. Simulation of Random Fields via Local Average Subdivision. *Journal of Engineering Mechanics*, 116(8):1733-1749.

Griffiths, D.V. and Fenton, G.A. 1993. Seepage beneath water retaining structures founded on spatially random soil. *Geotechnique*, 43(6):577-587.

Hsu, S.C. and Nelson P.P. 2006. Material spatial variability and slope stability of weak rock masses. *J. Geotech. and Geoenvir. Engrg,* 132(2):183–193.

Kozicki, J. and Donze, V.F. 2009. YADE-OPEN DEM: an open-source software using a discrete element method to simulate granular material. *Engineering Computations*, 26(7):786 – 805.

Schweiger, H.F. and Peschl, G.M. 2005. Reliability analysis in geotechnics with a random set finite element method. *Computers and Geotechnics*, 32:422–435.

Schweiger, H.F., Thurner, R., and Pöttler, R. 2001. Reliability analysis in geotechnics with deterministic finite elements – theoretical concepts and practical application. *Int J Geomech*, 14:389–413.

Suchomel, R. and Mašin, D. 2010. Comparison of different probabilistic methods for predicting stability of a slope in spatially variable c–φ soil. *Computers and Geotechnics*, 37(1-2):132-140.